A Precise Prediction of the Tooth Root Stresses for Involute External Gears with Any Fillet Geometry under Consideration of the Exact Meshing Condition

Tobias Paucker, Michael Otto and Karsten Stahl

Introduction

An efficient design with high power density characterizes a modern transmission, which leads, in many ways, to optimized constructions. Reaching a high utilization of material strength requires an exact prediction of occurring stress under given load carrying capacity to guarantee sufficient endurance.

Practically applied standardized methods to evaluate the load carrying capacity (AGMA 2101 (Ref. 1), DIN 3990 (Ref. 3), ISO 6336 (Ref. 4)) contain formulas to calculate the tooth root stress of standard profiles. At the same time, optimized profiles are designed that use more and more reserves of load carrying capacity (e.g. — optimized fillets, special tooth profile). Widely available FEM-calculations provide precise stress results, but are still laborious to apply for tooth contact analysis. Detailed, but fast and easy to use calculation methods are necessary to evaluate different types of tooth profiles in consideration of freely designed fillets. In addition, a more detailed analysis of standard tooth root profiles is required to increase power density. Also in many cases, expecting the maximum load and critical root stress at the tangent point of 30° (DIN3990 (Ref.3), ISO 6336 Ref. 4)) or the Lewis-Parabola (AGMA (Ref. 1) is not always right (Ref. 2.)

This paper shows a method to calculate the occurring tooth root stress for involute, external gears with any form of fillets very precisely within a few seconds. The following parameter variation uses a 2-D boundary element model to receive the notch stresses of the fillets. These calculated stresses are linked to a high-quality analytical tooth contact analysis to consider the exact relations of the gear mesh. This algorithm is implemented in the FVA software *RIKOR* (Refs. 5–6). The introduced model also allows a calculation of the occurring tension and compression stresses along the whole fillet for different mesh positions.

Calculation Method

The following section describes the calculation method that extends the standardized method of ISO 6336 (Ref.4).

Declaration of supporting points. Initially, a declaration of the supporting points of the tooth flank and the field of action is necessary to describe the calculation method.

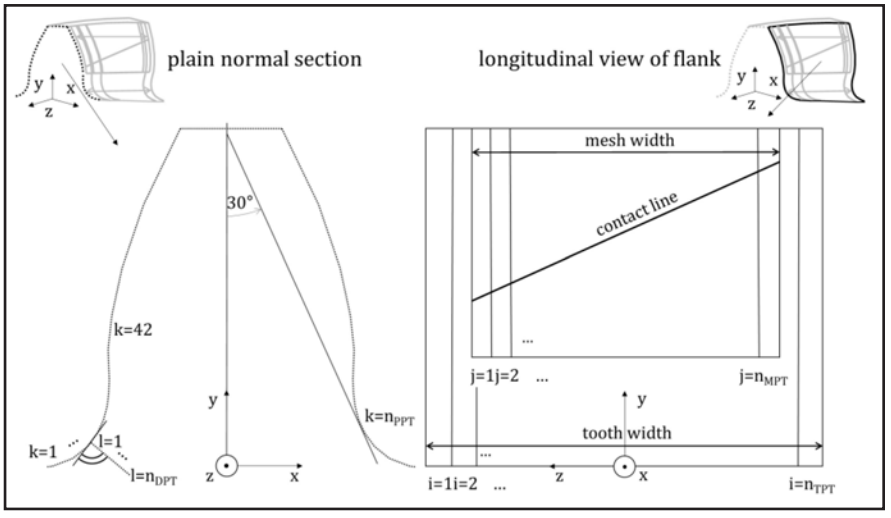

Figure 1 Definition of supporting points for a tooth and a contact line.

Figure 1 shows a definition of these supporting points for the plain normal section, and the plain longitudinal view of the tooth flank — including the root.

To illustrate the form of the fillet, it is most suitable to use a normal section of the tooth. For a spur gear, the normal and transverse sections are the same, located in a plane. But the normal section of a helical is curved in a 3-D area. To represent to actual fillet form precisely, a plain normal section is used. For later valuation, the plain normal section of the contour is indexed with a number of supporting points k (amount = n_{PPT}). At every point k of the contour, it is possible to define a number of supporting points l (amount = n_{DPT}) in normal direction to the inside of the gear material. For the analytical model, the tooth width is discretized in a number of supporting points i (amount = n_{TPT}). The mesh width is also discretized in a certain amount of supporting points j (amount = n_{MPT}), as it is not always the same size as the tooth width.

Figure 1 also shows the definition of a local coordinate system (x,y,z).

Influence function β_F of tooth root bending moment. To consider the tooth width and the bending lever, which varies in its longitudinal direction for helical gears, an influence function β_F is introduced that is based on investigations of Umezawa (Ref. 8).

This function describes the impact of a local tooth force at j to the bending moment, which occurs in i (compare to Eq. 1).

This paper was first presented at the International VDI Conference on Gears 2017, Garching/Munich [VDI-Berichte 2294, 2017, VDI Verlag GmbH] and is reprinted here with VDI approval.

When solving this function for a certain amount of supporting points and combining it with the local bending lever, a precise analytical calculation of the local bending moment (helical gears) is given.

$$\beta_{F_{i,j}} = \left(\frac{e^{-0.5 \cdot \left(\frac{z(i)-z(j)}{\sigma_\alpha \cdot h} \right)^2}}{\sqrt{2\pi} \cdot \sigma_\alpha} \right) \cdot \left(\frac{h_0}{h} \right) + S_{L_{i,j}} + S_{R_{i,j}}$$

β_F	[-]	Influence function of tooth root bending moment
i	[-]	Index of supporting point (tooth width)
z	[mm]	Coordinate in lead direction
h_0	[mm]	reference tooth height (1mm)
σ_α	[-]	Influence function of pressure angle
j	[-]	Index of supporting point (mesh width)
h	[mm]	Tooth height
$s_{l/r}$	[-]	Influence of edge

Equation 1: Calculation of the Influence function $\beta_{Fi,j}$ at supporting point *i* caused by a load acting on supporting point *j* based on Umezawa (8)

Tooth root bending moment M_i. While solving the influence function β_F for every discretized load on the contact line, the local tooth root bending moment M_i can be solved at every supporting point i (compare to Eq. 2). The local bending lever h_F is referenced to the boundary point of the 30°-tangent and the fillet. This method also allows the consideration of the exact load distribution.

$$M_i = \sum_{j=1}^{n_{MPT}} \beta_{F_{i,j}} \cdot h_{F_j} \cdot p_{F_j}$$

M_i	[N·mm]	Tooth root bending moment at supporting point i
i	[-]	Index of supporting point (tooth width)
β_F	[-]	Influence function of tooth root bending moment
p_F	[N]	Local tooth force
n_{MPT}	[-]	Number of supporting points (mesh width)
j	[-]	Index of supporting point (mesh width)
h_F	[mm]	Local bending lever to 30°-tangent

Equation 2: Calculation of the tooth root bending moment M_i at supporting point *i* with certain load distribution

Figure 2 shows the impact of a single load (left figure) on the tooth bending moment. Also shown is the effect of a certain load distribution and bending levers (right figure) on the occurring tooth bending moment and its allocation.

***Tooth root stress* σ_i.** Referring the bending moment to the bending section leads to the nominal tooth root stress of an equivalent beam (compare to Eq. 3). To consider the fillet it is possible to use the stress correction factor according to DIN 3990 (Ref. 3) or rather ISO 6336 (Ref. 4), which is referred to every loading point j. The calculated tooth root stress gives a maximum value without a specific declaration of the location of this stress. This stress correction factor does not allow considering any other root geometries than trochoids. The calculation of, e.g., grinding notches, asymmetric or otherwise optimized fillets is not possible. To determine the stress correction factor for such root geometries, it is necessary to calculate it with a numerical method.

$$\sigma_i = \frac{1}{W_b} \cdot \sum_{j=1}^{n_{MPT}} \beta_{F_{i,j}} \cdot h_{F_j} \cdot p_{F_j} \cdot Y_{S_j}$$

σ_i	[N/mm²]	Tooth root stress at supporting *point i*
i	[-]	Index of supporting point (tooth width)
β_F	[-]	Influence function of tooth root bending moment
p_F	[N]	Local tooth force
W_b	[mm³]	Bending section modulus at 30°-tangent
n_{MPT}	[-]	Number of supporting points (mesh width)
j	[-]	Index of supporting point (mesh width)
h_F	[mm]	Local bending lever to 30°-tangent
Y_S	[-]	Stress correction factor

Equation 3: Calculation of the tooth root stress σ_i at supporting point *i* with the exact load distribution p_{Fj} and the stress correction factor Y_{Sj} according to DIN 3990 (3) and ISO 6336 (4)

***Local stress correction factor* $Y_{Sj,k,l}$.** To allow the calculation of local stress correction factors for any fillet forms, it is convenient to use a numerical method. A 2-D numerical method is adequate to fulfill this requirement, while it also calculates very fast. Within this paper, a 2-D boundary element method (BEM) is used (Ref. 5).

The local stress correction factor $Y_{Sj,k,l}$ calculates for every location of the acting force j, along the fillet k, and also in normal direction to the inside of the gear l (surface tension also possible). It correlates to the quotient of a local tooth root stress at the investigated location and the reference bending stress at the equivalent beam (bending lever of acting force to the 30°tangent) (compare to Eq. 4).

This reference is necessary for this calculation method, but does not influence the calculation accuracy. A reference to every other tangent is possible as only the distribution between local stress correction factor and root bending moment would change, while their product would stay the same. The reference of the local stress correction factor is a certain load acting point j. Therefore, the stress-increasing effect of the fillet is constant along the mesh width for a certain load acting position.

$$Y_{S_{j,k,l}} = \frac{\sigma_{2D_{j,k,l}}}{\sigma_{2D,ref,j}}$$

$Y_{Sj,k,l}$	[-]	Local stress correction factor
k	[-]	Index of supporting point (profile)
σ_{2D}	[N/mm²]	Local tooth root stress with 2D numerical method
j	[-]	Index of supporting point (mesh width)
l	[-]	Index of supporting point (depth)
$\sigma_{2D,ref}$	[N/mm²]	Reference bending lever to 30°-tangent

Equation 4: Calculation of the local stress correction factor $Y_{Sj,k,l}$

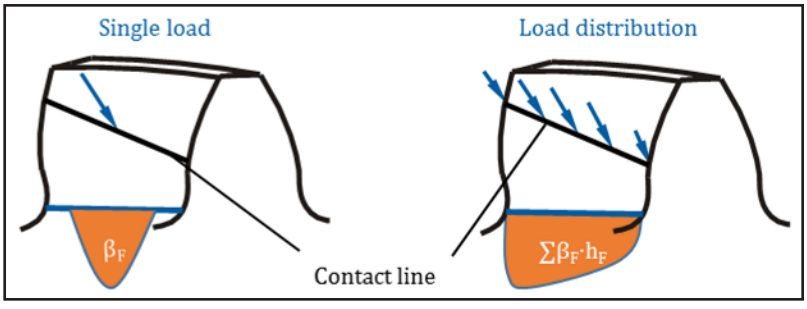

Figure 2 Illustration of the influence function β_F, local bending lever h_F and a certain load distribution p_F.

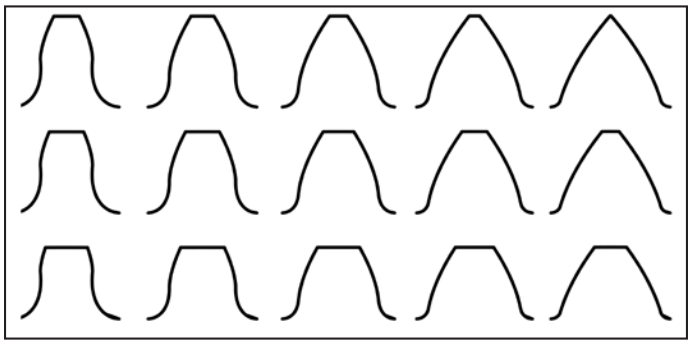

Figure 3 Tooth contours of varied parameters.

Table 1 Main geometry and 3-D model of investigated gear stage

3-D Model	Geometry	Gear 1	Gear 2	Unit
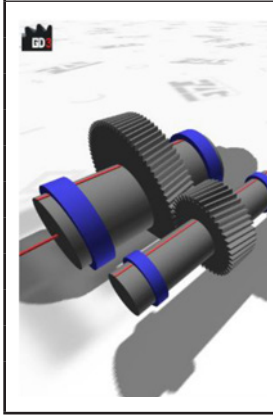	Module	1		mm
	Pressure angle	20		°
	Helix Angle	10	–10	°
	Number of Teeth	42	84	-
	Sum of profile shift	0		-
	Tip Diameter	*varies*		mm
	Root diameter	*varies*		mm
	Tooth width	18	18	mm
	Center distance	63.97		mm
	Contact ratio	*varies*		-
	Overlap ratio (nominal)	1.0		-

Table 2 Tool data and plain normal section of the investigated gear stage

Plain normal secion of gear 1	Tool Data	Gear 1	Unit
	Add. coeff. basic rack	1.5	-
	Ded. coeff. basic rack	1.6	-
	Tip radius	0.25	-
	Generating profile shift of this case	0 (*varies*)	-
	Protuberance angle	-	°
	Depth of protuberance	-	mm

Local tooth root stress $\sigma_{i,k,l}$**.** With exchanging the standardized stress correction factor with the local and numerical determined stress correction factor, it is possible to calculate a local tooth root stress at any location of the fillet (Eq. 5). This method also allows the prediction of the location of the highest occurring root stresses. With the requirement of very low calculation time, it would also be convenient to use this algorithm for optimizations. Within this paper it is used to compare the results to the standardized approach of ISO 6336 (Ref. 4).

$$\sigma_{i,k,l} = \frac{1}{W_b} \cdot \sum_{j=1}^{n_{MPT}} \beta_{F_{i,j}} \cdot h_{F_j} \cdot p_{F_j} \cdot Y_{S_{j,k,l}}$$

$\sigma_{i,k,l}$	[N/mm^2]	Tooth root stress at supporting point *i*
i	[-]	Index of supporting point (tooth width)
k	[-]	Index of supporting point (profile)
β_F	[-]	Influence function of tooth root bending moment
p_F	[N]	Local tooth force
W_b	[mm^3]	Bending section modulus at 30°-tangent
n_{MPT}	[-]	Number of supporting points (mesh width)
j	[-]	Index of supporting point (mesh width)
l	[-]	Index of supporting point (depth)
h_F	[mm]	Local bending lever to 30°-tangent
Y_S	[-]	Stress correction factor

Equation 5: Calculation of the local tooth root stress $\sigma_{i,k,l}$ at supporting point *i*, profile point *k* and depth point *l* with the exact load distribution p_{Fj} and the local stress correction factor $Y_{S_{i,k,l}}$

Parameter Variation and Results

The calculation method, introduced above, allows doing extensive parameter variations and studies and comparing the results to, e.g., standardized methods. In the following, a parameter study is shown, which investigates different trochoid fillet geometries and compares them to the corresponding results of ISO 6336 (Ref. 4). The variations are made with very stiff shafts and bearings, as the influence of these machine elements are not in focus for these calculations. The influence of the mesh stiffness is considered for these calculations.

Varied parameters. There are different possibilities to change the fillet geometry. The presented calculation study shows a variation of the profile shift x ($-1 \le x \le 1$) and the tooth height h_a (influences contact ratio $-1 \le \varepsilon_\alpha \le 1$). A different tooth height leads to changing contact ratio and, therefore, a variation of the critical contact line that is responsible for the maximum tooth root stress. The sum of profile shift is zero for every case to keep

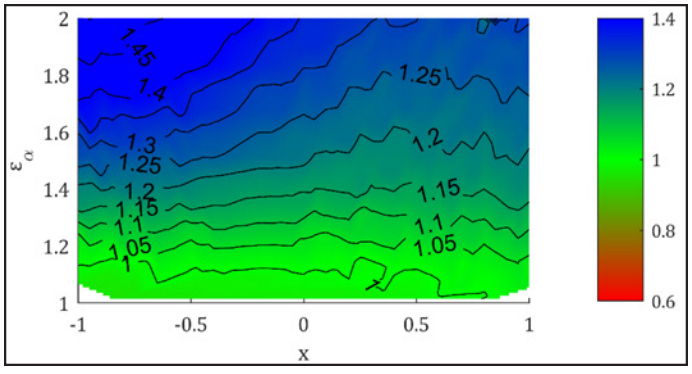

Figure 4 Relation of maximum tooth root stress σ_i according to ISO 6336 (Ref. 4) to maximum local tooth root stress $\sigma_{i,k,l}$ according to Eq. 5.

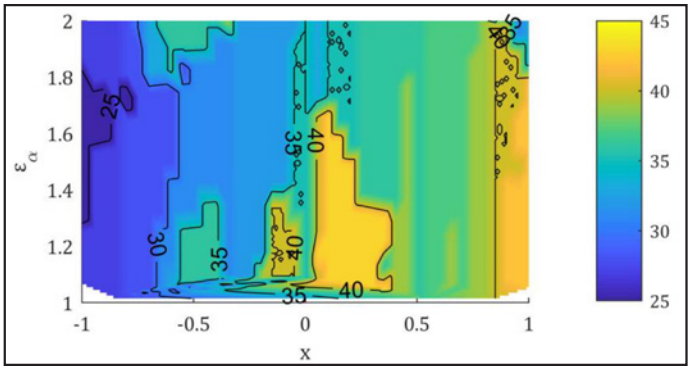

Figure 5 Location (in ° of tangent) of the maximum local tooth root stress $\sigma_{i,k,l}$ according to Eq. 5.

the same center distance. The plane normal sections of the different investigated tooth contours are shown (Fig. 3), while the focus of the calculations lies on the pinion ($z = 42$).

Table 1 shows the 3-D model with the geometrical data of the gears, and Table 2 shows the tool data for gear 1 of this model.

Influence of the contact ratio. Figure 4 shows the relation of the maximum tooth root stress according to ISO 6336 (Ref. 4) to the maximum tooth root stress according to Equation 5. A result above one means that the calculation according to ISO 6336 (Ref. 4) gives higher results as the local method of this paper. A main result is that for increasing contact ratios, the standardized method calculates very safely. Schinagl (Ref. 7) investigates the influences of the profile and contact ratio within his dissertation, while his results support this consideration.

Location of maximum tooth root bending stress. The method also allows an investigation of the location of the maximum occurring stress. The reference stress of the corresponding beam is at the 30°-tangent. Figure 5 shows the location (in ° of the tangent) of the maximum tooth root stress, depending on the profile shift and the contact ratio (critical contact line). With an increasing profile shift, the radius of the fillet decreases. The critical tension stress gets shifted nearer to the center of the tooth root fillet, which may lead to a more critical alternating load.

Further Calculation Possibilities

The discussed geometries of the variation are focusing on trochoid fillet geometries. Of course, the numerical method is not restricted to certain root geometries. Therefore, there are different calculations imaginable that are introduced in the following section. The pros and cons of each fillet geometry — especially of optimized forms — are not discussed.

Calculation of grinding notches. For case hardened gears, it is common to manufacture them with a certain amount of protuberance and finish the gears with a grinding process after hardening. An unfavorable behavior can be the occurrence of grinding notches. To evaluate these fillets forms there are different approaches, such as the investigations of grinding notches by Wirth (Ref. 9). To determine an exact or even measured contour, the approaches, which only describe the notches or protuberances analytically, are not promising. More productive is an investigation of the exact fillet form with numerical methods. Figure 6 shows a nominal contour compared to one with a grinding notch. An important point is to be able to evaluate these kinds of manufacturing deviations and to be able to react in an adequate amount of time without having to run extensive tests. Figure 8 shows a calculation of a gear with a grinding notch (normal section of the contour and tangential stresses); the 3-D illustration is shown for one tooth within Figure 9.

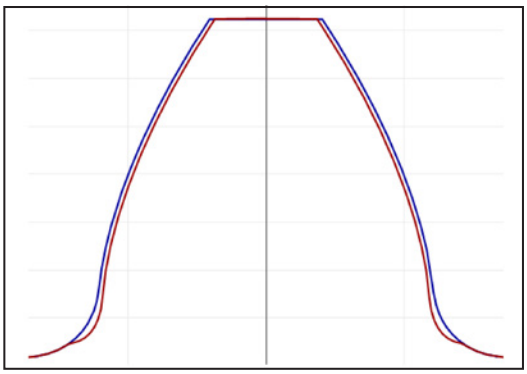

Figure 6 Nominal contour (outer, blue contour) and contour with grinding notch (inner, red contour).

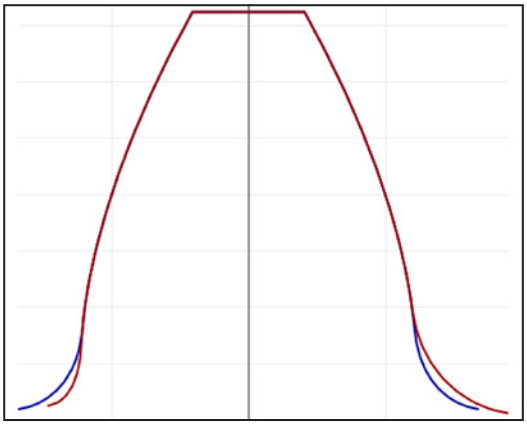

Figure 7 Nominal contour and asymmetric tooth root contour.

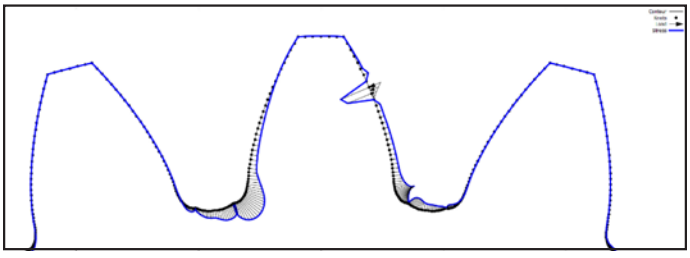

Figure 8 Illustration of the tangential stresses in plain normal section of protuberance (upper figure) and grinding notches (lower figure) on local tooth root stresses.

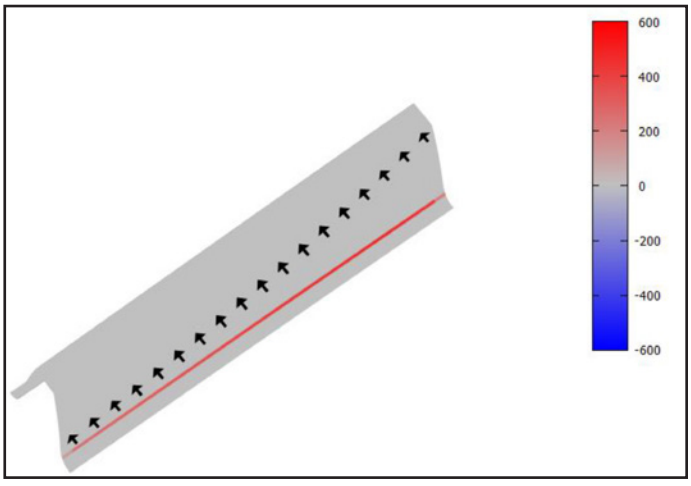

Figure 9 Illustration for one tooth of 3-D calculation of local tooth root stress $\sigma_{i,k,l}$ (along the certain tangent in N/mm^2) for full contact line of a helical gear (compression side is covered by the tooth flank)

Calculation of asymmetric root geometries. The critical tooth root stress according to DIN 3990 (Ref. 3) and ISO 6336 (Ref. 4) is represented as a tension at the side of the acting load. Therefore, it is possible to reduce the radius of the tooth root at the compression side in order to allow a wider radius at the side of the tension. An example of such an asymmetric root contour is shown (Fig. 7). To evaluate this sort of optimization it is possible to use the introduced algorithm. The distribution of the root stresses can be seen (Fig. 10) for a load acting at both sides.

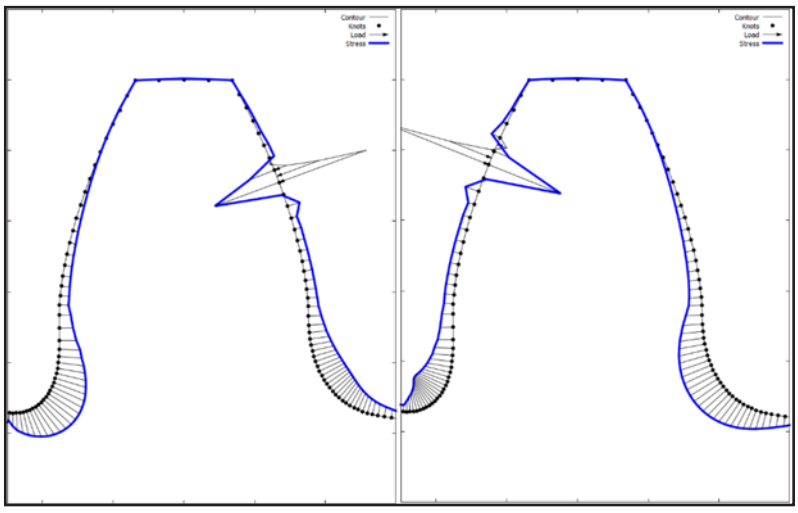

Figure 10 Asymmetric root geometry with load acting at sharp (right figure) and wide radius (left figure).

Conclusion

This paper introduces an algorithm to calculate precisely and quickly the local tooth root stress for involute external gears with any fillet geometry, and under consideration of the exact meshing condition. The formulas for this method and an extensive variation are introduced that show deviations between the simpler standardized approach and the presented local approach. A main result is that the standardized method according to ISO 6336 (Ref. 4) calculates the occurring maximum tension stress very safely for high contact ratios. By using this method the material utilization can be increased by up to 50%. The location of the maximum tooth stress deviates significantly for different profile shifts. Furthermore, examples of calculations for any root geometries are shown. On the one hand, with optimized fillet forms it is possible to decrease the occurring stresses up to 30%. On the other hand, an evaluation of manufacturing deviations is possible without test runs. All examples are calculated without the influences of shafts and bearings, which would lead to more unequal load sharing.

Future investigations should also cover these influences, as an unequal load sharing does not lead to an unequal stress distribution within the same amount. In addition, the introduced algorithm is suitable for root optimizations with any fillet geometry. To discuss and exercise this fact, further investigations are necessary.

For more information. Questions or comments regarding this paper? Contact Tobias Paucker at *paucker@fzg.mw.tum.de*.

References

1. AGMA (Hrsg.): AGMA 2101. Fundamental Rating Factors and Calculation Methods for Involute Spur and Helical Gear Teeth, AGMA, 2004.
2. Börner, J. and H. Linke. Örtliche Fußspannung, FVA-Heft 492, FVA e.V., Frankfurt a. M., 1996.
3. DIN (Hrsg.): DIN 3990 Teil 1-6. Tragfähigkeitsberechnung von Stirnrädern, Beuth Verlag, 1987.
4. ISO (Hrsg.): ISO 6336. Calculation of Load Capacity of Spur and Helical Gears, Genf, 2006.
5. Paucker, T. W. Wagner, M. Otto, M. Senf, S. Schumann, K. Stahl and B. Schlecht. "Berechnungsmodul Örtliche Zahnfußspannung," FVA-Heft 1246, Frankfurt a. M., 2017.
6. Paucker, T., W. Wagner, M. Otto, M. Senf, M., S. Schumann, K. Stahl and B. Schlecht. "Berechnungsmodul Ortliche Zahnfußspannung," FVA-Informationsblatt, Frankfurt a. M., 2017.
7. Schinagl, S. Zahnfußtragfähigkeit Schrägverzahnter Stirnräder unter Berücksichtigung der Lastverteilung," Diss. TU München, 2002.
8. Umezawa, K. "The Meshing Test on Helical Gears under Load Transmission," 2nd Report; "The Approximate Formula for Bending-Moment Distribution of Gear Tooth," *Bulletin of the JSME,* 1973.
9. Wirth, X. "Über den Einfluss von Schleifkerben Oberflächengehärteter Zahnräder auf die Dauerfestigkeit und die Lebensdauer im Zweistufenversuch," Diss. TU München, 1977.

Tobias Paucker works as a Research Associate at the Gear Research Centre (FZG) at the Technical University of Munich.

Dr. Michael Otto joined FZG in 2000 as a research assistant and gained his position as head of department in 2006. He holds a Ph.D. in mechanical engineering; the topic of his research activities were load distribution and tooth root carrying capacity. Current research activities include gear geometry, tooth contact analysis and gearbox-related NVH. Another main focus is deformation and stress analysis of supporting shafts and bearings in the gearbox. He drives the development of various scientific programs that are available for companies that are members of FVA (German Research Association for Gears and Transmissions). He is also head of department — Calculation and Verification of Transmission Systems — at the Gear Research Center (FZG), chaired by Prof. K. Stahl, TU München.

Prof. Dr. Karsten Stahl is Chair, Machine Elements, Mechanical Engineering, at TUM. He leads and conducts research in the area of mechanical drive systems, with particular interest in investigating the load capacity, efficiency and dynamics of all gears types. His other areas of interest include applications in automotive engineering such as synchronization systems and multi-disc clutches. Stahl has developed methods for analysis that have been incorporated into international standards, together with the component strength values derived by means of these methods. He studied mechanical engineering at TUM and performed his doctoral studies from 1994 to 2000 in the Machine Elements Department. In 2001, he joined BMW, first as a gear development engineer, then as the manager of gear development in Dingolfing. In 2006 he transferred to the MINI plant in Oxford where he was initially quality manager for transmissions, then quality manager for powertrains and suspensions. In 2009 he took over responsibility for the initial development and innovation management of powertrain and vehicle dynamics systems at BMW in Munich. Stahl has been a full professor in the Machine Elements Department since 2011.